Liquid Crystals
Publication details, including instructions for authors and subscription information:
http://www.informaworld.com/smpp/title~content=t713926090

Flexoelectric response at defect sites in nematic inversion walls

Pramoda Kumar[a]; K. S. Krishnamurthy[a]
[a] Centre for Liquid Crystal Research, Jalahalli, Bangalore 560 013, India

To cite this Article Kumar, Pramoda and Krishnamurthy, K. S.(2006) 'Flexoelectric response at defect sites in nematic inversion walls', Liquid Crystals, 33: 2, 131 — 138
To link to this Article: DOI: 10.1080/02678290500473669
URL: http://dx.doi.org/10.1080/02678290500473669

Liquid Crystals, Vol. 33, No. 2, February 2006, 131–138

Flexoelectric response at defect sites in nematic inversion walls

PRAMODA KUMAR and K.S. KRISHNAMURTHY*
Centre for Liquid Crystal Research, PO Box 1329, Jalahalli, Bangalore 560 013, India

(*Received 8 August 2005; accepted 7 October 2005*)

Electric field experiments have been carried out on +1 and −1 defects formed in alignment inversion walls, in a planarly aligned nematic phenyl benzoate. The results show that the defects are non-singular in the core and exhibit a flexoelectric response to an applied d.c. or low frequency a.c. field. When the *c*-director flux lines are circular, as in a +1 defect in a wall parallel to the easy axis, flexoelectro-optic switching characterized by an azimuthal angle variation is observed. When the *c*-director flux is radial, the response is seemingly through polar angle variations involving no rotation of the extinction brushes due to crossed polarizers. This conclusion follows from the field-induced structural distortions observed at a −1 defect having a combination of radial and tangential *c*-director fields.

1. Introduction

A strain-free nematic is invariant with respect to an inversion of its director, $\mathbf{n} \rightarrow -\mathbf{n}$. Curvature deformations of the splay and bend type could break this symmetry and lead to a non-vanishing local polarization of the medium [1]. Following the sign convention in [2], the polarization density $\mathbf{P}$ corresponding to this so-called flexoelectric effect may be written as

$$\mathbf{P} = e_S\, \mathbf{n}(\nabla \cdot \mathbf{n}) + e_B\, \mathbf{n} \times (\nabla \times \mathbf{n})$$

where e_S and e_B are the flexoelectric coefficients appropriate to the splay and bend distortions, respectively. Flexoelectric polarization may arise from a coupling between molecular shape asymmetry and permanent dipolar moments [1]; it may also be due to an asymmetry in the way the electric quadrupoles assemble in the presence of curvature strains [3].

Under certain conditions, an inverse flexoelectric effect is produced in which an applied electric field generates a curvature strain of the splay, bend or splay–bend type in a nematic. A few years ago, Rudquist *et al.* [4] reported inverse flexoelectric distortions in twisted bipolar nematic droplets. They explained their observations on the basis of a flexoelectro-optic phenomenon [5] in which the optical axis of a helical structure rotates about the direction of a static field orthogonal to it. Our study deals with electric field-induced structural distortions that occur at +1 and −1 defects in alignment inversion walls, in a planarly aligned nematic phenyl benzoate. Because of curvature distortions associated with defect structures, flexoelectric charge separation is inherent in them; however, in the absence of an external electric field, for symmetry reasons, there may be no net polarization. Application of the field could disturb the symmetry and produce a net polarization along the field so as to minimize the free energy. We demonstrate that the field driven structural changes at defect sites could in general involve changes in both azimuthal and polar angles defining the local director. In particular, under an electric field normal to the sample plane (or along the defect line), a net flexoelectric polarization is generated solely through polar angle variations when the initial field lines of the *c*-director (or sample plane component-director) are radial; and through azimuthal angle variations when they are circular or tangential.

2. Experimental

We used a reagent grade sample of butyl 4-(4-

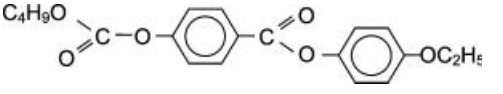

ethoxyphenoxycarbonyl)phenyl carbonate (BEPC) supplied by Eastman Organic Chemicals. It exhibited an enantiotropic nematic phase between *c*. 55 and 84°C. The sample cells were sandwich type, constructed of ITO-coated glass plates. Mylar spacers, heat-sealed to the electrodes through cooling from *c*. 250°C under a uniform pressure, determined the cell spacing, *d*. The

*Corresponding author. Email: kristy@vsnl.net

Liquid Crystals
ISSN 0267-8292 print/ISSN 1366-5855 online © 2006 Taylor & Francis
http://www.tandf.co.uk/journals
DOI: 10.1080/02678290500473669

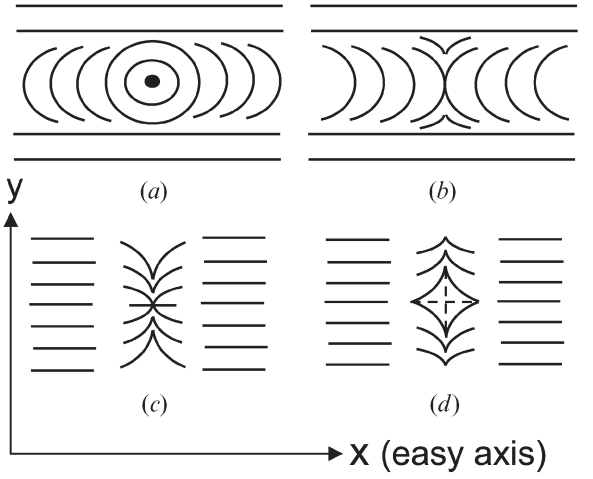

Figure 1. Singular points in surface walls at which wedge disclination lines emerge. (*a*) and (*b*) correspond, respectively, to +1 and −1 defects in a wall along the easy axis; (*c*) and (*d*), to +1 and −1defects in a wall normal to the easy axis.

d-value was determined interferometrically, using the channelled spectrum. For securing a planar alignment, the electrodes were rubbed unidirectionally on silk prior to cell construction and no surfactant material was used. The rubbing or easy direction fixes the reference axis x. The alignment was quite uniform over the entire sample area (~1.5 cm × 1 cm), except at the defect sites; this was evident from the total extinction of light in the defect-free regions observed between crossed polarizers with their transmission axes along x and y. Observations were carried out in transmitted light, along z, the layer normal, using a Leitz DMRXP polarizing microscope, equipped with a Sony CCD camera and a Mettler FP90 hot stage. The electric field was applied along $\pm z$. The voltage source was a Stanford Research Systems DS 345 function generator coupled to a FLC Electronics voltage amplifier (Model F20ADI). The applied voltage was measured with a HP 34401A multimeter.

The value of dielectric anisotropy, $\Delta\varepsilon$, for BEPC has been reported as varying from about 0.21 at the melting temperature to 0.06 at 84°C [6]. The results of our independent dielectric measurements on BEPC agreed with the reported data to within 5%. The resistivity of BEPC at 75°C was $\sim 5 \times 10^9\,\Omega$cm. The birefringence of BEPC has been reported as ranging between 0.141 at 56°C and 0.087 at 83°C [7].

For convenience, when the polarizer has its transmission axis along x and the analyser along y, it will be represented as P(x)-A(y); P(45)-A(135) indicates diagonal setting of polarizer and analyser, with the angles in parentheses in degrees measured from the x-direction.

3. Results and discussion

3.1. *Wall stability*

Nematic layers aligned planarly between unidirectionally rubbed plates often exhibit narrow inversion walls containing several linear defects normal to the sample plane [8]. Such walls are expected to be stable only at the limiting surfaces and to smear out in bulk as this would reduce the energy [9]. However, wedge disclination lines situated at surface singularities could prevail also in the bulk, as schematically shown in the director patterns in figure 1 [10]. With freshly prepared thin (~5 µm) BEPC samples, we found even the inversion walls to be stable for long periods, of the order of days. In figure 2 (*a*) we reproduce an inversion wall containing a few linear defects of strength ± 1, as seen between crossed polarizers, P(x)-A(y). With a tilting compensator B introduced diagonally as in figure 2 (*b*), evidently, compensation is obtained along that side of the wall where the director is normal to the slow direction ($n \perp \gamma$) of the compensator. The corresponding retardation is about 450 nm which also happens to be the path difference for the aligned background region displaying a first order brown in the figure. The second order green bands in figure 2 (*b*) outline the path along which the

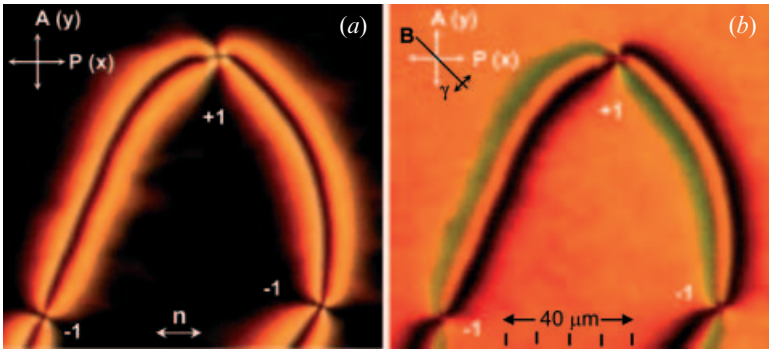

Figure 2. An alignment inversion wall at 66°C with linear defects of strength ± 1. (*a*) Between crossed polarizers; (*b*) with a tilt compensator B set for zero retardation along either side of the wall.

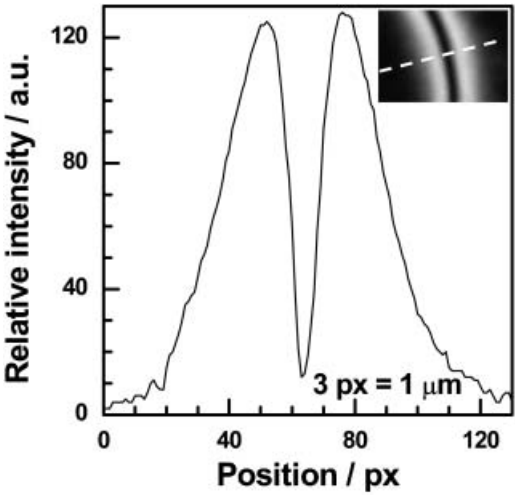

Figure 3. A typical intensity profile across wall-thickness, obtained using the grey-scale image of the wall in figure 2 (*a*); it corresponds to the broken white line in the inset showing a section of the wall.

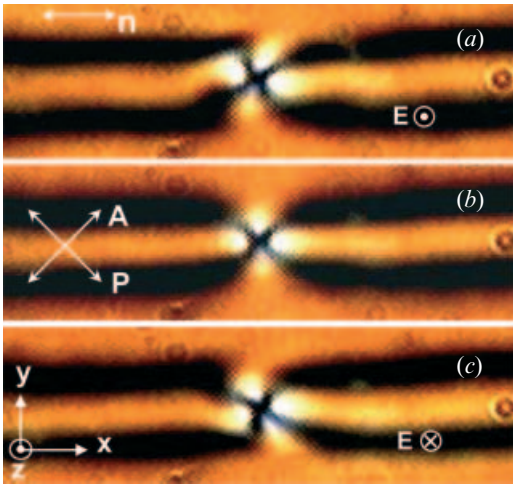

Figure 4. Appearance of a +1 defect in a horizontal wall, between diagonally crossed polarizers. Applied bias is +5 V in (*a*), 0 V in (*b*) and −5 V in (*c*). The sample is 4.6 μm thick, at 70°C; picture sizes $50 \times 16.7\,\mu m^2$.

director is parallel to the slow direction of B. These observations indicate that the wall is a bulk one. This is hardly surprising considering that the wall is much thicker than the nematic layer, measuring about 10 μm between its opposite diagonally oriented director regions, as evident from the intensity profile in figure 3; the penetration of the surface order at the two substrates into the bulk appears adequate to render the wall metastable. A reduction in the order of birefringence colours in the wall region becomes perceptible only after the sample is several days old.

3.2. *Flexoelectro-optic switching at a +1 defect in a wall along the easy axis*

Figure 4 (*b*) shows the section of a wall parallel to *x* in which a +1 defect is formed. At the defect site, the birefringence colour has fallen from brown of the first order to white of the same order, corresponding to a retardation change by about 250 nm. This indicates that the core of the defect is nonsingular in bulk. Accordingly we modify the director configuration in figure 1 (*a*) to include a twist deformation as in figure 5. On application of a d.c. field, the extinction cross at a given defect is observed to rotate clockwise or anticlockwise, depending on the field direction, as in figures 4 (*a*) and 4 (*c*). Further, for the same field direction, the rotation sense at different +1 defect sites is found to be non-uniform in general; that is, if it is clockwise at one site, it could be the opposite at another. We could detect the switching effect down to about 0.8 V. With a low frequency a.c. field, it is noticeable at even lower voltages. The extent of rotation is found to be linear in field, indicating its flexoelectric origin. In fact, these observations are very similar to those of Rudquist *et al.* [4] on twisted bipolar nematic droplets formed of achiral molecules. Structurally, in such droplets the director is twisted about both horizontal

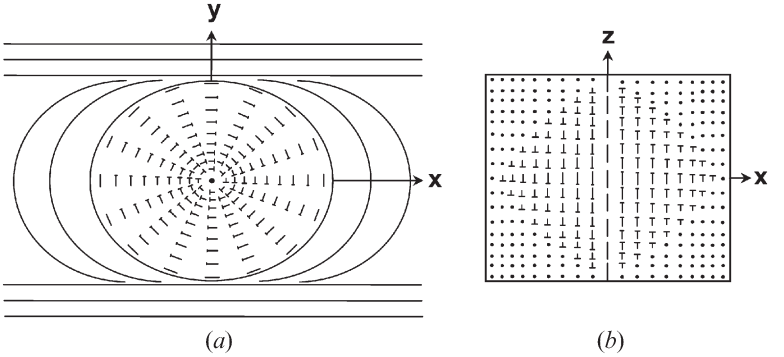

Figure 5. The director field at a +1 defect. (*a*) Midplane $z=0$; (*b*) vertical section $y=0$.

and vertical directions. In the case of a +1 defect, the twist occurs only about the horizontal and the substrate orientations are approached primarily through splay–bend deformations, as in figure 5 (*b*). Nevertheless, as in bipolar droplets, the basic mechanism of field-driven deformation here is the flexoelectro-optic phenomenon, first recognized by Patel and Meyer in the course of their electro-optic studies on cholesterics [5]. Briefly, as earlier noted, it refers to the rotation of the local director in cholesterics about the direction of an electric field applied transverse to the helix axis; it produces a periodic splay–bend curvature in the director field and thereby a net flexoelectric polarization along the field direction. Thus a reduction in free energy is achieved.

For a +1 disclination along z, the director configuration normal to z is described by the well known equation [8]

$$\varphi = \tan^{-1}(y/x) + \alpha$$

where φ is the angle with respect to x of the director confined to the xy-plane and α is a constant angle; α represents the deviation of the director (or tangent to the flux line) at any point from the line through the defect centre and that point. Constancy of α implies that the flux lines are in general logarithmic spirals degenerating into radial lines for $\alpha = n\pi$, and to circles, for $\alpha = n\pi/2$, n being an integer. The $z=0$ plane structure of *a* +1 defect with a non-singular core, as in figure 5, corresponds to the case of $\alpha = \pi/2$, with an added director twist about the radial direction. In the field-on state, if α is altered by a constant quantity, say β ($\ll \pi/2$), the midplane projections of the director outline logarithmic spirals as in figure 6. It is easy to see that in the vertical plane through any spiral arm, the director conforms to a splay–bend pattern with a concomitant vertical flexoelectric polarization. The sign of β is decided by the sign of the flexoelectric coefficient $e = (e_S + e_B)/2$, helix wave vector k and the applied field **E**. Since k has equal probability of being positive or negative in a given defect, the sign of β need not be uniform for different defects of the same type. For cholesterics, the angle β through which the optic axis (or the helix axis) rotates is shown [5] to be given by

$$\tan\beta = \frac{eE}{Kk} = \frac{eEp}{2\pi K}$$

where K is the average of splay and bend elastic constants, and p is the helical pitch. From a separate measurement on volume flexobands [11] in BEPC, we obtained e/K as ~0.3 per volt. With $\beta \approx 20^\circ$ for $\mathbf{E} = 1.087\,\mathrm{V\,\mu m^{-1}}$, we obtain the diameter of the defect (corresponding to a half turn helix) as equal to about 3.5 μm. From figure 4, it is clear that this value is about 4–5 times smaller than the actual size. The reason for this apparent anomaly is probably the decrease in helix pitch with increase in vertical distance from the midplane. The pitch variation renders the logarithmic spirals three dimensional and consequently an extension to a +1 defect of flexoelectro-optic equations applicable to cholesterics cannot be fully justified.

At elevated voltages (>6 V), volume flexoelectric distortion appears in the entire sample in the form of a periodic system of bands, parallel to the easy axis and regularly spaced along y. The bands are the so-called (θ, φ) bands arising in planar samples subject to rigid boundary conditions; they are due to a periodic

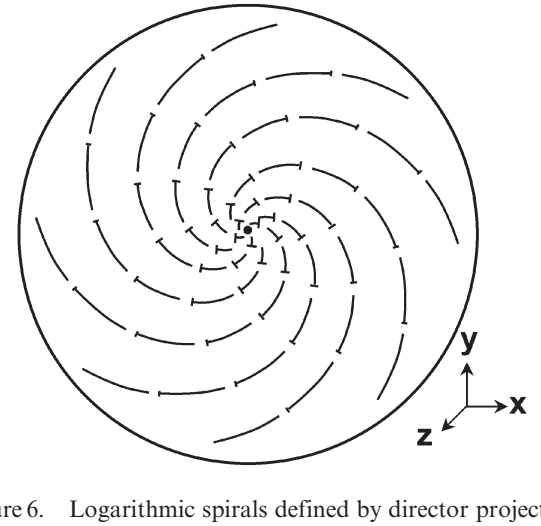

Figure 6. Logarithmic spirals defined by director projections in the $z=0$ plane. A splay–bend arc pattern of alignment is present in any vertical plane (Bouligand plane [6]) containing opposite spiral arms. This configuration is for **E** along z, $e>0$ and an initially right handed helical structure ($k>0$), as in figure 5.

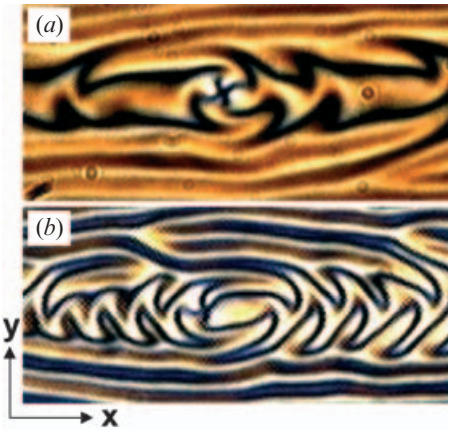

Figure 7. Photographs showing volume flexobands that form along the easy axis at elevated voltages. (*a*) 7 V, (*b*) 14 V, 70°C. With this instability, the wall turns zigzag while the extinction brushes assume a spiral geometry.

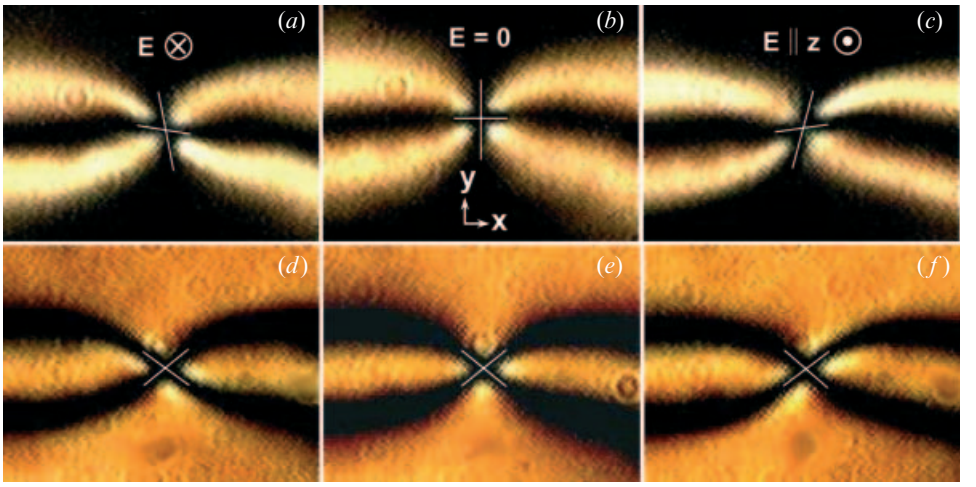

Figure 8. Appearance of a −1 defect in a horizontal wall. P(x)-A(y) for (*a–c*); P(45)-A(135) for (*d–f*). Voltage is 0 in (*b*) and (*e*); −5 V (**E** inward) in (*a*) and (*d*); +5 V in (*c*) and (*f*); 70°C. Crossed white lines indicate brush orientations.

variation of these angles along the y-direction in any given xy-plane [11]. With the onset of this instability the inversion walls undergo a zigzag distortion; the defects in the wall remain stable while the extinction brushes assume a spiral geometry, as seen in figure 7. Interestingly, along each of the spiral brushes in this figure, the angular position of extinction is seen to increase with the radial distance.

3.3. *Flexoelectric switching at a −1 defect in a wall parallel to the easy axis*

The nature of switching of extinction brushes at a −1 defect is significantly different from that at a +1 defect. With the setting P(x)-A(y), the horizontal and vertical brushes are observed to rotate in opposite senses, in a scissoring fashion, under a d.c. field; their sense of rotation reverses with the field, as in figures 8 (*a*) and 8 (*c*). On the other hand, with P(45)-A(135), hardly any rotational motion of the brushes is noticed in the field-on state, as is evident from figures 8 (*d–f*). However, subtle variations in texture indicate orientational changes. For instance, one of the diagonal brushes becomes narrower relative to its zero field width; but the other diagonal brush widens, as in figure 8 (*d*). The effect is opposite when the field is reversed, as seen in figure 8 (*f*). Similarly, the position of reduced birefringence colours appearing between the brushes —whitish yellow spots in figures 8 (*d–f*) — alters on application of field.

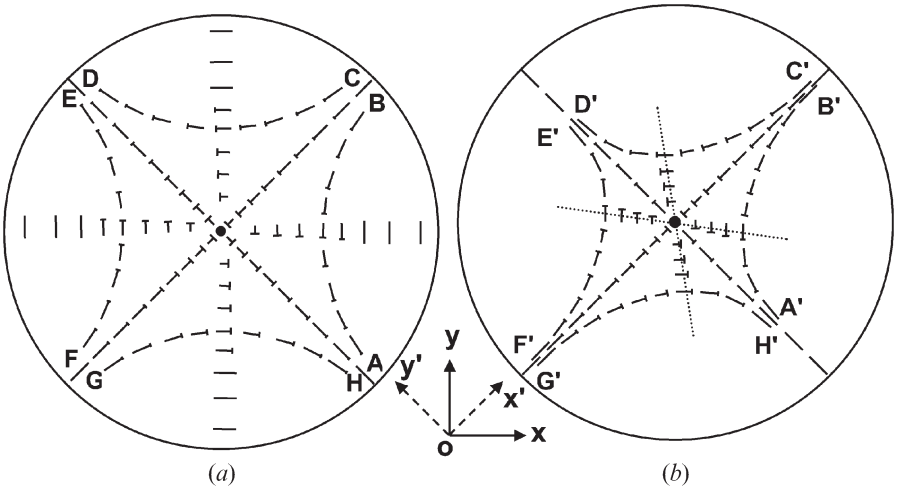

Figure 9. (*a*) Director field in the midplane z=0 for a −1 defect formed in an inversion wall parallel to easy axis; **E**=0. (*b*) Changed director field for **E**>0, considering polar tilt variations along x' and y'; the dotted lines indicate the extinction brush positions for P(x)-A(y); and the pattern corresponds to observations in figure 8 (c, f).

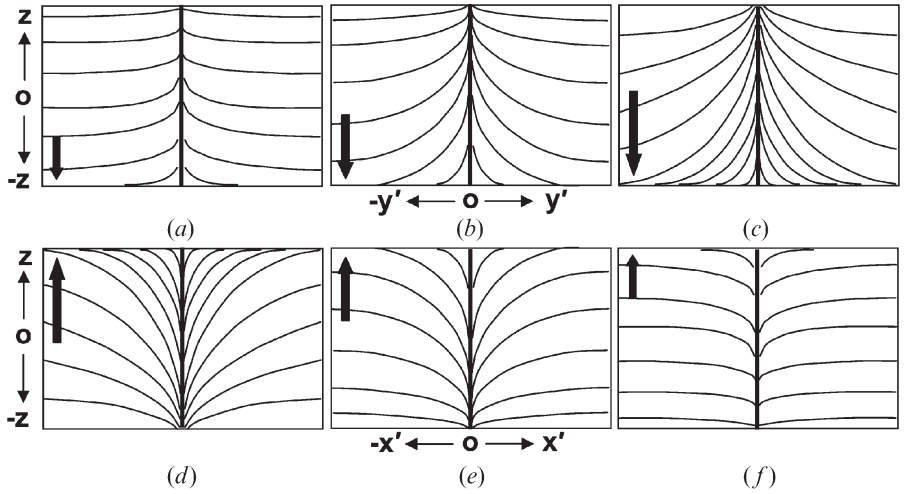

Figure 10. Schematic representation of the director field in $x'z$- and $y'z$-planes containing the defect line. Field $\mathbf{E}=0$ for (b),(e); $\mathbf{E}>0$ along, say, z, for (a), (d); $\mathbf{E}<0$ for (c), (f). Black arrows are schematics of flexoelectric polarization in each case. Net polarization exists only in the on state.

To explain these observations, we may begin by considering the initial director field. As in the case of a +1 defect, the core of a −1 defect is rendered non-singular by incorporating out-of-plane tilts in the configuration represented by figure 1 (b); the modified pattern is shown in figure 9 (a). In considering the effect of an applied field, we readily recognize that the flexoelectro-optic phenomenon cannot be the sole mechanism of distortion here. While brush rotations as in figures 8 (a, c) indicate a change in azimuthal angle along the x- and y-directions, width variations of diagonal brushes as in figures 8 (d, f) signify changes in polar angle along x' and y'. If the initial director orientation referred to (x, y, z) is given by ($\sin\theta\cos\varphi$, $\sin\theta\sin\varphi$, $\cos\theta$), φ is 45° along x' and 135° along y'; introducing θ-variations of opposite sign for the x'- and y'-directions in the field-on state, we arrive at the director field presented in figure 9 (b). This would result in a net polarization parallel to the applied field as in figure 10. Further, referring to the director trace on the xy-plane as the c-director, the c-director flux lines between the asymptotes (x', y') are, as shown in figure 9 (a), equilateral hyperbolae, in the field-free state. Consequent on θ-variation along (x', y') there will be φ-variations in other directions so that the c-director flux lines lose their original equilateral symmetry, as indicated in figure 9 (b). Essentially the same conclusion is arrived at by considering flexoelectro-optic rotation of the helix axes along x and y. The change in equilateral hyperbolic flux lines brought about by this rotation is schematically shown in figure 11. Consequent asymmetry in the splay–bend structure leading to a non-vanishing polarization is illustrated in figure 12.

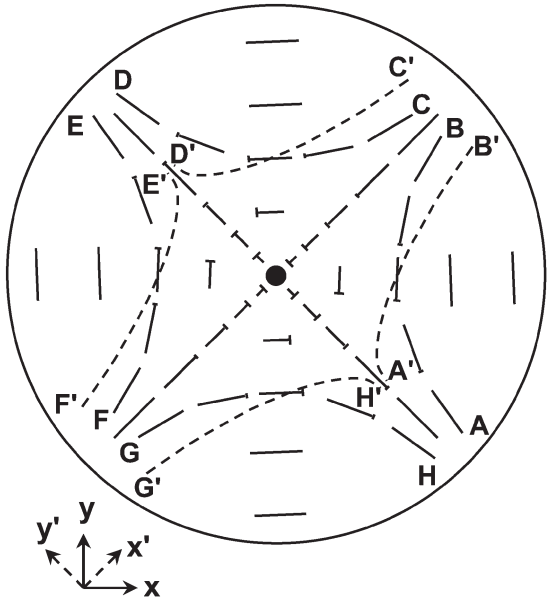

Figure 11. Director field at the site of a −1 defect, with the nail heads emerging outward. AB, CD. EF and GH are representative equilateral hyperbolic vertical planes involving similar splay–bend distortions in the initial state. The dotted lines indicate the shift in these planes in the field-on state.

With crossed polarizers P(x)-A(y), we measured the angle of rotation Ω of one of the extinction brushes (that parallel to y) as a function of the applied field. Flexoelectric origin of the rotation is again indicated by the near linear scaling of Ω with the field as evident from figure 13.

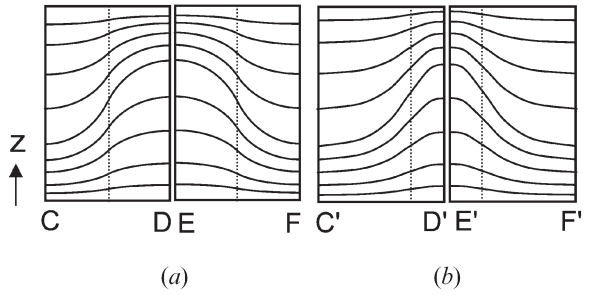

Figure 12. (*a*) Director flux lines in vertical planes through equilateral hyperbolae CD and EF, for **E**=0; symmetry of splay–bend distortion results in the absence of flexopolarization. (*b*) Change in flux lines for **E**≠0 leading to an asymmetry in the splay-bend pattern and a net polarization.

3.4. *Flexoelectric switching at a −1 defect in a wall normal to the easy axis*

The director field corresponding to a −1 defect located in a wall parallel to the *y*-axis is obtained simply by rotating the configuration in figure 9 (*a*) through 45° about the defect line. Accordingly, the switching behaviour in the present case is expected to be similar to that discussed in the previous section. In figure 14 we present the observed results. In the field-on state, with the polarizers set diagonally as P(45)-A(135), the extinction brushes display a scissoring type of rotational motion corresponding to flexoelectro-optic-like rotation occurring along diagonal directions (x', y'). For the setting P(x)-A(y), the brushes show no rotational motion, but display changes in their width corresponding to θ-variations along x and y.

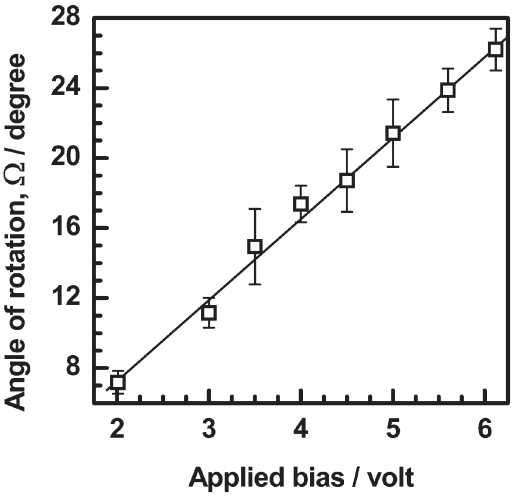

Figure 13. Angle of rotation of the vertical extinction brush of a −1 defect in a horizontal wall as a function of applied bias. Electrode separation is 4.6 µm, 77°C.

4. Concluding remarks

Linear defects and anti-defects of unit strength that form in alignment inversion walls are non-singular in the core and exhibit a flexoelectric response to an applied d.c. or low frequency a.c. field. When the *c*-director flux is circular, as in a +1 defect located in a wall along the easy

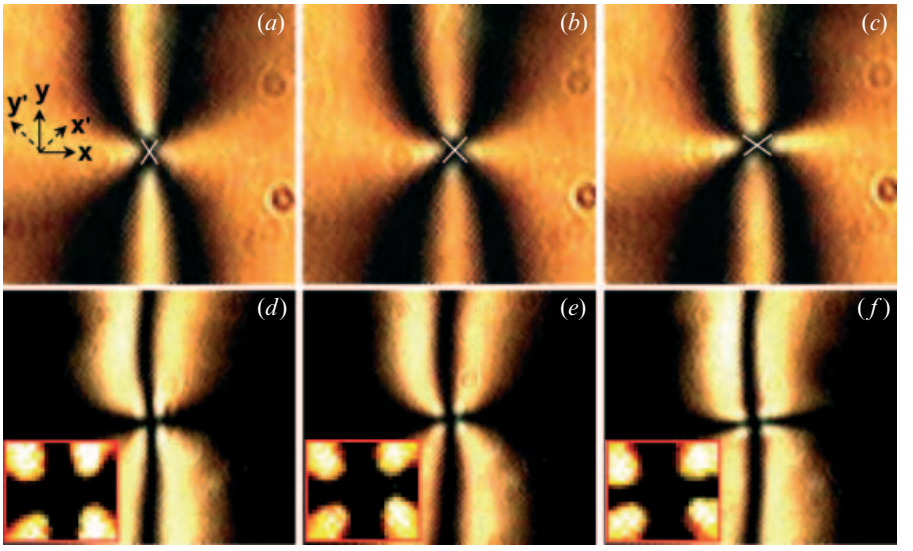

Figure 14. A −1 defect in a π-wall along *y*. Crossed polarizers; P(45)-A(135) for (*a–c*); P(x)-A(y) for (*d–f*). Applied bias is +4.2 V in (*a*), (*d*); 0 V in (*b*), (*e*); −4.2 V in (*c*), (*f*). The white lines in (*a–c*) indicate extinction brush orientations. 70°C. 4.6 µm thick sample. The insets within the red borders in (*d–f*) are the magnified and contrast-enhanced images corresponding to the central zones of extinction brushes. In (*f*), compared with (*e*), the vertical brush is wider and the horizontal one narrower; the situation in (*d*) is the reverse.

axis, the response is similar to that observed for twisted bipolar achiral nematic drops [4] and involves the flexoelectro-optic phenomenon. When the *c*-director field is radial, as in a +1 defect in a wall normal to the easy axis, only polar angle variations are expected. It must be mentioned that in the many samples studied, we were unable to find a defect of this type. However, −1 defects which involve both radial and tangential *c*-director fields, are observed to exhibit an electro-optic response consistent with this conclusion.

Acknowledgements

We are indebted to Professor N. V. Madhusudana (Raman Research Institute, Bangalore) and Dr S. Krishna Prasad (Centre for Liquid Crystal Research, Bangalore) for many useful discussions.

References

[1] R.B. Meyer. *Phys. Rev. Lett.*, **22**, 918 (1969).
[2] P. Rudquist, S.T. Lagerwall. *Liq. Cryst.*, **23**, 503 (1997).
[3] J. Prost, J.P. Marcerou. *J. Phys. Fr.*, **38**, 315 (1977).
[4] P. Rudquist, E. Korblova, D.M. Walba, R. Shao, N.A. Clark, J.E. Maclennan. *Liq. Cryst.*, **26**, 1555 (1999).
[5] J.S. Patel, R.B. Meyer. *Phys. Rev. Lett.*, **58**, 1538 (1987).
[6] W.H. de Jeu, Th.W. Lathouwers. *Mol. Cryst. liq. Cryst.*, **26**, 225 (1974).
[7] D. Balzarini, P. Palffy-Muhoray. *Liquid Crystals, and Ordered Fluids* Vol. 4, A.C. Griffin, J.F. Johnson (Eds), pp. 531, Plenum Press, New York (1984).
[8] J. Nehring, A. Saupe. *J. chem. Soc. Faraday Trans. II*, **68**, 1 (1972).
[9] P.G. de Gennes, J. Prost. *The Physics of Liquid Crystals*, 2nd Edn, pp. 166, Clarendon Press, Oxford (1993).
[10] M. Kleman, C. Williams. *Phil. Mag.*, **28**, 725 (1973).
[11] S.A. Pikin. *Structural Transformations in Liquid Crystals*, pp. 175–189, Gordon and Breach, New York (1991).